# TWO-DIMENSIONAL MODELLING OF SOFT FERROMAGNETIC FILMS

ANTONIO DESIMONE,[1] ROBERT V. KOHN,[2] STEFAN MÜLLER,[1]
FELIX OTTO,[3] AND RUDOLF SCHÄFER[4]

ABSTRACT. We examine the response of a soft ferromagnetic film to an in-plane applied magnetic field by means of both theory and experiment. In the thin-film limit, we uncover a separation of scales in the rough energy landscape of micromagnetics: leading order terms generate constraints which eliminate degrees of freedom, terms of second order in the film thickness lead to a (new) reduced variational model, higher order terms are related to wall, vortex, and anisotropy energies. We propose a new strategy to compute low-energy domain patterns, which proceeds in two steps: we determine first the magnetic charge density by solving a convex variational problem, then we construct an associated magnetization field using a robust numerical method. Experimental results show good agreement with the theory. Our analysis is consistent with prior work by van den Berg and by Bryant and Suhl, but it goes much further; in particular it applies even for large fields which penetrate the sample.

## 1. INTRODUCTION

Soft ferromagnetic films are of great interest both for applications and as a model physical system. Their sensitive response to applied magnetic fields makes them useful for the design of many devices, including inductive or GMR sensors, and magnetoelectronic memory elements [1]. Therefore soft thin films have been the object of much experimental and computational study [2]. The large variety of relatively simple domain patterns they display makes such films a convenient paradigm for analyzing the microstructural origin of magnetic hysteresis. More generally, they provide a crucial example for studying the response of systems evolving through the multiplicity of metastable states resulting from a rough energy landscape [3].

Most current modeling of soft thin films is based on direct micromagnetic simulation [4], [5]. This is demanding due to the long-range

*Date*: Leipzig, February 18, 2001.

nature of dipolar interactions, and to the necessity of resolving several small length scales simultaneously. Numerical simulation is surely the right tool for the quantitative study of hysteresis and dynamic switching [6], [7]. However it is natural to seek a more analytical understanding of the equilibrium configurations. The origin of domain patterns is intuitively clear: they arise through a competition between the magnetostatic effects (which favor pole-free in-plane magnetization) and the applied field (which tends to align the magnetization). A two-dimensional model based on this intuition was developed by van den Berg [8] in the absence of an applied field, and extended by Bryant and Suhl [9] to the case of a sufficiently weak in-plane applied field. In van den Berg's model magnetic domain patterns are represented using two-dimensional, unit-length, divergence-free vector fields, determined using the method of characteristics; the caustics where characteristics meet are domain walls. In Bryant and Suhl's model, the presence of a weak applied field is accounted for through an electrostatic analogy: the "charges" associated with the magnetic domain pattern should be such as to expel the applied field from the interior of the sample, as occurs in an electrical conductor. The domain patterns predicted by Bryant and Suhl have, in fact, been observed experimentally [11]. The electrostatic analogy is restricted, however, to sufficiently small applied fields: since the magnetization vector has a constrained magnitude, the field generated by its divergence cannot be arbitrarily large. Therefore Bryant and Suhl's model breaks down at a critical field strength beyond which the external field penetrates the sample.

This paper extends and clarifies the models described above. Our extension is two-fold: we permit large applied fields which penetrate the sample, and we replace the method of characteristics with a robust numerical scheme. Our clarification is also two-fold: we identify the regime in which these two-dimenasional models are valid and, while providing them with a variational formulation, we explain their relation to classical micromagnetics. Indeed, the energy functional of the dimensionally reduced model is the thin film limit (in the sense of gamma-convergence [12]) of the three-dimensional energy functional of micromagnetics. In this respect, our work extends previous results of Gioia and James in this direction [13]. Finally, to assess our proposed model, we compare its predictions to experiments on Permalloy thin film elements with square cross-section. The agreement between theory and experiment is remarkable, even in the field penetration regime.

At a more fundamental level, this paper is a contribution to the study of systems governed by rough energy landscapes. At the heart of our approach is an asymptotic analysis of the micromagnetic energy in

the thin-film limit. This limit process reveals a hierarchical structure in the energy, which separates into low-order terms, "essential part", and higher-order terms. The low-order terms lead to constraints (e.g. the component of the magnetization along the thickness direction must vanish), hence to the elimination of degrees of freedom. The essential part is the term of second order in the film thickness: It leads to a (new) reduced variational principle which sets the charge density. Wall energies and anisotropy contribute only at higher order. The higher-order terms are not irrelevant: they provide the energy barriers which are the source of magnetic hysteresis. Moreover, they break the degeneracy in the reduced theory. Our analysis indicates, however, that in spite of the non-uniqueness of domain patterns, certain quantities (namely, the charge density, the region of field penetration, and the magnetization in the penetrated region) are uniquely predicted by the reduced model and should have little or no hysteresis.

## 2. Micromagnetics: from Three to Two Dimensions

The free-energy functional of micromagnetics in units of $J_s^2 L^3/2\mu_0$ is

$$\begin{aligned} E_d(m) &= (\kappa d)^2 \int_{\Omega_d} |\nabla m|^2 dx + Q \int_{\Omega_d} \varphi(m) dx \\ &+ \int_{\boldsymbol{R}^3} |h_d|^2 dx - 2 \int_{\Omega_d} h'_e \cdot m dx \,. \end{aligned} \tag{2.1}$$

Here $m$ is the magnetization (in units of the saturation magnetization $J_s$), a unit vector field defined on the film $\Omega_d$ with cross section $\omega$ and thickness $d$, where all lengths are measured in units of a typical lateral dimension $L$ (the diameter for $\omega$ a circle, the edge-length for $\omega$ a square). Moreover, $\kappa$ is the ratio between exchange length $D_{BL}$ and film thickness, where $D_{BL} = (2\mu_0 A/J_s^2)^{\frac{1}{2}}$, and $A$ is the exchange constant; $Q$ is the quality factor measuring the strength of the magnetic anisotropy $\varphi$ relative to that of dipolar interactions; $h_d$ is the stray field in units of $J_s/\mu_0$, and the corresponding integral is the magnetostatic energy; $h'_e$ is the applied field in units of $J_s/\mu_0$, which we assume to be uniform and parallel to the film's cross section. In what follows, a prime will always denote a two-dimensional field or operator.

For $d \ll 1$ a hierarchical structure emerges in the energy landscape of (2.1), see Table 2.1, as it can be checked with direct calculations. Variations of $m$ of order one along the thickness direction $x_3$ give rise to an exchange energy per unit area (of the cross section) of order $\kappa^2 d$. An out–of–plane component $m_3$ of order one determines a magnetostatic contribution per unit area of order $d$. The component of the in-plane

TABLE 2.1. Scaling of various energy sources

| | |
|---|---|
| $\frac{\partial m}{\partial x_3}$ | $\kappa^2 d$ |
| $m_3$ | $d$ |
| $[m' \cdot \nu']$ | $\ln(\frac{1}{d})\, d^2$ |
| $\mathrm{div}' m'$ | $d^2$ |
| external field energy | $h'_e\, d$ |
| anisotropy energy | $Q\, d$ |
| asymmetric Bloch wall | $\kappa^2\, d^2$ |
| Néel wall | $(\ln(\frac{1}{\kappa^2 d}))^{-1}\, d^2$ |
| vortex | $\ln(\frac{1}{\kappa\, d})\, \kappa^2\, d^3$ |

magnetization $m'$ orthogonal to the lateral boundary $\partial\omega$ of the film's cross section $\omega$ leads to a magnetostatic contribution of order $d^2 \ln \frac{1}{d}$ per unit length. The same mechanism penalizes jumps $[m' \cdot \nu']$ of the normal component of the magnetization across a line of discontinuity of $m'$ with normal $\nu'$. These lines of discontinuity arise by approximating domain walls as sharp interfaces. At order $d^2$ we find the magnetostatic energy per unit area due to surface "charges" proportional to the in-plane divergence $\mathrm{div}' m'$. Finally, the energy per unit length of a Néel or asymmetric Bloch wall and the energy of a single vortex are indicated in the table. In the regime

$$H'_e = \frac{h'_e}{d} \sim 1, \quad \frac{Q}{d} \ll 1, \quad d \ll \kappa^2 \ll \frac{1}{d \ln\left(\frac{1}{d}\right)}\,, \tag{2.2}$$

the low-order terms penalizing $m_3$, $\frac{\partial m}{\partial x_3}$ and $[m' \cdot \nu']$ become hard constraints, while the energetic cost of anisotropy, of the wall type of minimal energy[1], and of vortices become higher-order terms. The energy is thus determined, at principal order, by the competition between the aligning effect of $H'_e$ and the demagnetizing effects due to $\mathrm{div}' m'$.

In view of this separation of energy scales in the regime (2.2), the following reduced theory emerges naturally. We call an in–plane vector field $m'(x')$ on $\omega$ "regular" if it satisfies $[m' \cdot \nu'] = 0$ across all possible discontinuity lines and at $\partial\omega$. Our reduced theory states that the magnetization $m'(x')$ minimizes

$$E(m') = \int_{\boldsymbol{R}^3} |H_d|^2\, dx - 2 \int_\omega H'_e \cdot m'\, dx', \tag{2.3}$$

[1]Note that (2.2) probes a range of film thicknesses over which different wall types are to be expected, see ref. [2]. Typical values of the material parameters for Permalloy are $Q = 2.5 \times 10^{-4}$ and $D_{BL} = 5$nm. Thus, for a circular element with diameter 1 $\mu$m and thickness 10 nm we have $d = 0.01$ and $\kappa = 0.5$.

where $H_d(x) = -\nabla U$ is determined by

$$\begin{aligned} \nabla^2 U &= 0 \text{ in } \mathbb{R}^3 \text{ outside of } \omega, \\ \left[\frac{\partial U}{\partial x_3}\right] &= \mathrm{div}' m' \text{ on } \omega, \end{aligned}$$

among all regular in-plane vector fields $m'$ of unit length

$$|m'| = 1 \text{ in } \omega. \tag{2.4}$$

Our formula for the induced field $H_d$ is naturally consistent with that commonly used for two-dimensional micromagnetic simulations [15]. In fact, the argument in support of our reduced theory is not only based on heuristics. We have actually proved gamma-convergence of the energy functional (2.1) to (2.3), but the technical (and rather lengthy) arguments which are required to establish this result are beyond the scope of the present paper, and will be published elsewhere [14].

We now make two crucial observations. (i): the functional $E$ depends on $m'$ only via the surface charge $\sigma = -\mathrm{div}' m'$, and it is strictly convex in $\sigma$. Indeed, $\int_{\mathbb{R}^3} |H_d|^2 \, dx$ is a quadratic functional of $\sigma$ and an integration by parts shows that $\int_\omega H_e' \cdot m' \, dx'$ is a linear functional of $\sigma$. (ii): for any regular $m_0'$ of at most unit length, that is

$$|m_0'| \le 1 \text{ in } \omega, \tag{2.5}$$

there exist many regular $m'$ of unit length with the same surface charge: $\mathrm{div}' m' = \mathrm{div}' m_0'$. Indeed, we may write $m' = \nabla^\perp \psi + m_0'$ where $\nabla^\perp \psi = (-\partial\psi/\partial x_2, \partial\psi/\partial x_1)$ and the continuous function $\psi(x')$ on $\omega$ solves the boundary value problem

$$|\nabla^\perp \psi + m_0'| = 1 \text{ in } \omega, \tag{2.6}$$

$$\psi = 0 \text{ on } \partial\omega. \tag{2.7}$$

One can generate many solutions by imposing the additional condition $\psi = 0$ on an arbitrary curve contained in $\omega$.

These observations have two important consequences. First, the minimizer of the reduced energy $E$ is not uniquely determined. Indeed, according to (i), $E$ depends only on the surface charge, and according to (ii), a regular in–plane vector field of unit length is not uniquely determined by its surface charge. The second consequence is that the surface charge and thus the stray field are uniquely determined. Indeed, according to (i), $E$ is a strictly convex function of the surface charge, and according to (ii), the set of surface charges which can be generated by regular in–plane vector fields of unit length is convex. (This is true despite the fact that the set of regular in–plane vector fields with unit length is not convex.)

Any minimizer $m'$ of (2.3,2.4) satisfies the Euler-Lagrange equation

$$H'_d + H'_e = \lambda\, m' \ \text{ in } \omega, \tag{2.8}$$

where $\lambda(x')$ is the Lagrange multiplier associated with the pointwise constraint (2.4). Since $H_d$ is uniquely determined, the region $\{H'_d + H'_e \neq 0\}$ of $\omega$ where the external field is not expelled from the sample is uniquely determined. Within this penetrated region, $m'$ is also uniquely determined in view of (2.8).

There exists a finite critical field strength $H_{crit}$, in the following sense: when the applied field is subcritical, $\lambda \equiv 0$ and the field is completely expelled from the sample, whereas when it is supercritical $\lambda$ is nonzero somewhere and the field penetrates in that part of the sample. The critical field strength depends on the geometry of $\omega$ — for a circular disk of diameter one, its value is one.

## 3. Computation of Domain Patterns within the Reduced Theory

To derive quantitative predictions from our reduced model (2.3,2.4), we proceed in two steps. The first step minimizes (2.3) among all regular in–plane vector fields $m'_0$ of length *less than or equal to* 1. Recall that replacing (2.4) by (2.5) does not change the minimum energy; therefore the $m'_0$ obtained this way has the correct reduced energy, though it typically violates (2.4). The second step postprocesses $m'_0$ by solving (2.6,2.7) to obtain another minimizer $m'$ of unit length. This $m'$ is the desired magnetization.

The first step is a convex (though degenerate) variational problem. We solve it using an interior point method [16]. More in detail, the convex constraint is enforced by adding to the physical energy $E$ a small multiple $t$ of a self–concordant barrier $B$. The unique stationary point of (the strictly convex) $E + tB$ is computed by Newton's method; it serves as an initial guess for the minimizer of $E + t'B$, where $t' < t$. The parameter $t$ is then slowly decreased by multiplicative increments. Within Newton's method, the Hessian of $E + tB$ is inverted by a preconditioned conjugate gradient method, where the magnetostatic part of the Hessian is evaluated with the help of Fast Fourier Transform.

For the second step, we recall that the solution of (2.6,2.7) is not unique. However there is a special solution $\psi$, known as the "viscosity solution", which has special mathematical properties [17]. It is robust and can be computed efficiently using the "level set method" [18]. This is what we compute.

Our numerical scheme selects — automatically and robustly — one of the many minimizers $m'$. The selection principle implicit in this

scheme is the same as the one proposed by Bryant and Suhl. It appears to pick a minimizer with as few walls as possible. Thus it is not unlike the more physical selection mechanism of minimizing wall energy, represented as a higher-order correction to (2.3) [19], [20]. More complex configurations of (presumably) higher energy (in particular, remanent states showing more intricate wall structures) can also be generated, easily but not automatically, by setting $\psi = 0$ on curves contained in $\omega$.

Figure 3.1 shows the predictions of our numerical scheme for a square film of edge-length one, subject to a monotonically increasing field applied along the diagonal. This rather special geometry was chosen to guarantee that nontrivial domain patterns could persist beyond field penetration, as illustrated by the 90-degree domain wall emerging from the bottom right corner of the sample. To check our predictions, we have observed the response of two ac-demagnetized Permalloy ($Ni_{81}Fe_{19}$, $J_s = 1.0$ T) square samples of edge lengths $L = 30$ and 60 $\mu$m and thicknesses $D = 40$ and 230 nm, respectively, in a digitally enhanced Kerr microscope. The observed domain patterns are given in Figures 3.2, 3.3 where the field intensity $h_e$, measured in Tesla, is scaled according to

$$H = \frac{L}{D}\frac{h_e}{J_s}. \tag{3.1}$$

In comparing Figures 3.1, 3.2, and 3.3 one may speculate that the small lag in the strength of the applied field exhibited by the thinner samples may be due the fact that, for these films, the walls are of Néel type and they are repelled by the lateral boundary (an $\ln(\frac{1}{d})\, d^2$ effect, according to Table 2.1). This effect could be captured by an enhanced two-dimensional model in which higher-order terms in the film thickness are taken into account.

Figure 3.4 examines more closely the predictions of our theory for $|H_e'|$ near $H_{crit}$. We have superimposed on each gray-scale plot the level curves of the potential $v$ of the penetrated field, defined by $-\nabla v = H_d' + H_e'$. Regions where the field lines concentrate are regions where $\nabla v \neq 0$, i.e., where the external field has penetrated the sample. Within them, (2.8) implies that $m'$ is parallel to $\nabla v$ . Our theory predicts that $m'$ can have no walls in the penetrated region. The pictures confirm this, and show quite clearly that two apparently independent phenomena – the expulsion of the domain walls from the interior of the sample and the penetration of the external field – are in fact two manifestations of the same event.

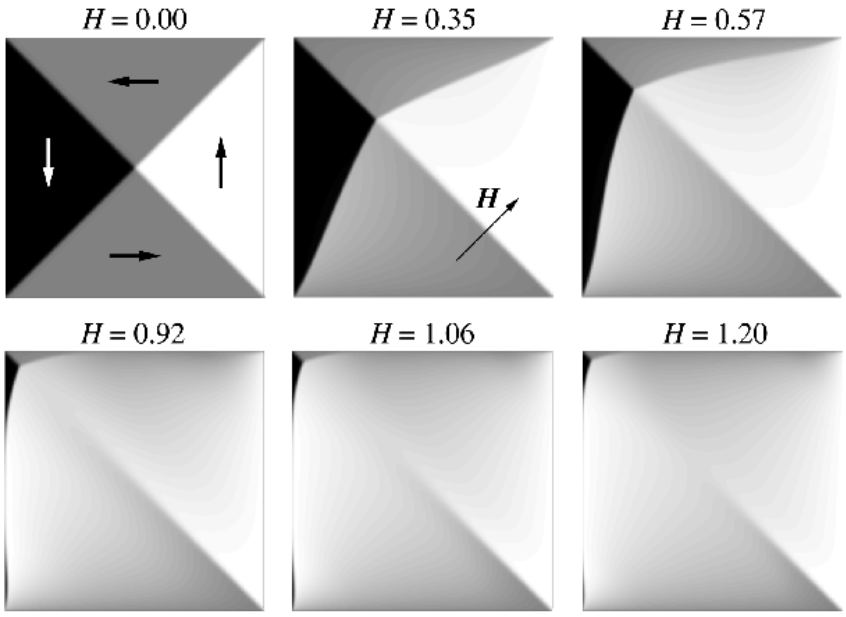


FIGURE 3.1. Predictions of the theory: gray-scale plots of the vertical component of magnetization.

## 4. Discussion

In summary, our model describes the response of a soft ferromagnetic thin film to an applied magnetic field. It determines the micromagnetic energy to principal order, and certain associated physical quantities that should have little or no hysteresis — the charge density, the region of field penetration, and the magnetization in the penetrated region. In addition our scheme provides a specific magnetization pattern which is consistent with experimental observation and may well be the ground state. Of course, the magnetization of a soft thin film is not uniquely determined by the applied field: the multiplicity of metastable states is a primary source of hysteresis. Our reduced model simplifies the energy landscape: among the many micromagnetic equilibria, only those with low energy survive, and they can be computed effectively. Our approach does not yet provide a model for hysteresis or a classification of stable structures, but it does suggest a strategy of attack, namely, through the analysis of higher-order terms in the micromagnetic energy.

## Acknowledgements

We thank Sergio Conti for valuable discussions and suggestions.

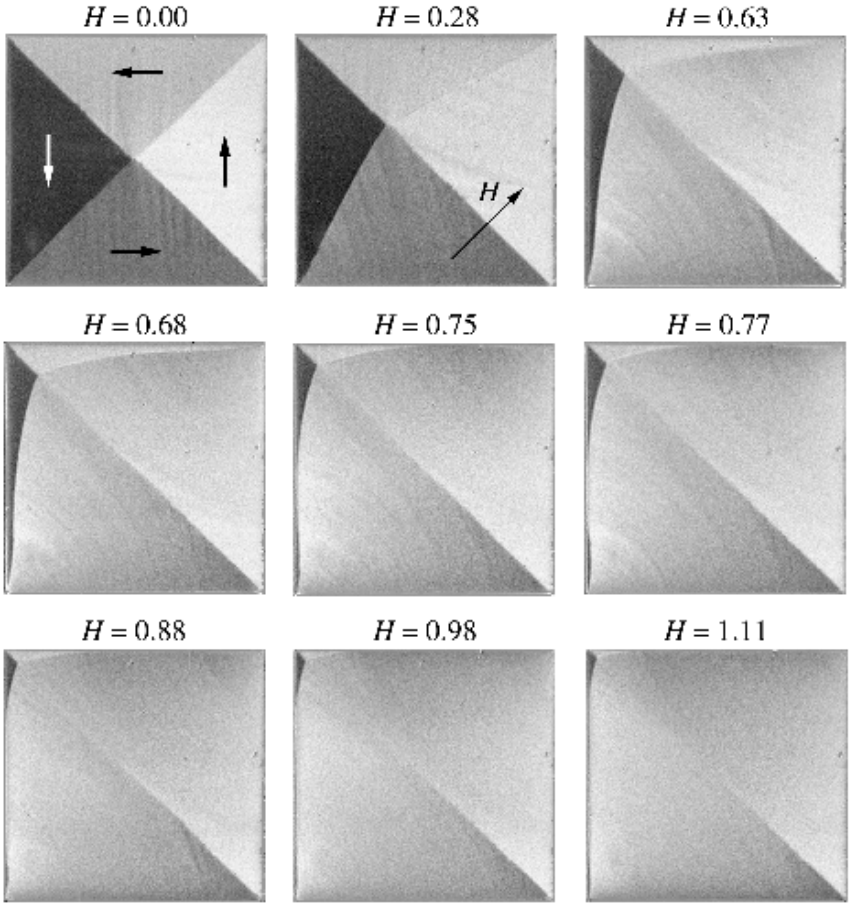


FIGURE 3.2. Permalloy films: $L = 60$ $\mu$m, $D = 230$ nm.

## REFERENCES

[1] Physics Today, special issue on magnetoelectronics, **48** (1995).
[2] A. Hubert and R. Schäfer, *Magnetic Domains* (Springer, Berlin–Heidelberg–New York, 1998).
[3] G. Bertotti, *Hysteresis in Magnetism* (Academic Press, San Diego, 1998).
[4] J. Fidler, T. Schrefl, K. Kirk, and J.N. Chapman, Domain structures and switching mechanisms in patterned magnetic elements, J. Magnetism Magn. Mat. **175**, 193 (1997).
[5] J.G. Zhu, Y. Zheng, and X. Lin, Micromagnetics of small size patterned exchange biased Permalloy film elements, J. Appl. Phys. **81**, 4336 (1997).
[6] R.H. Koch, J.G. Deak, D.W. Abraham, P.L. Trouilloud, R.A. Altman, Yu Lu, W.J. Gallagher, R.E. Scheuerlein, K.P. Roche, and S.S.P. Parkin, Magnetization reversal in micron-sized magnetic thin films, Phys. Rev. Lett. **81**, 4512 (1998).

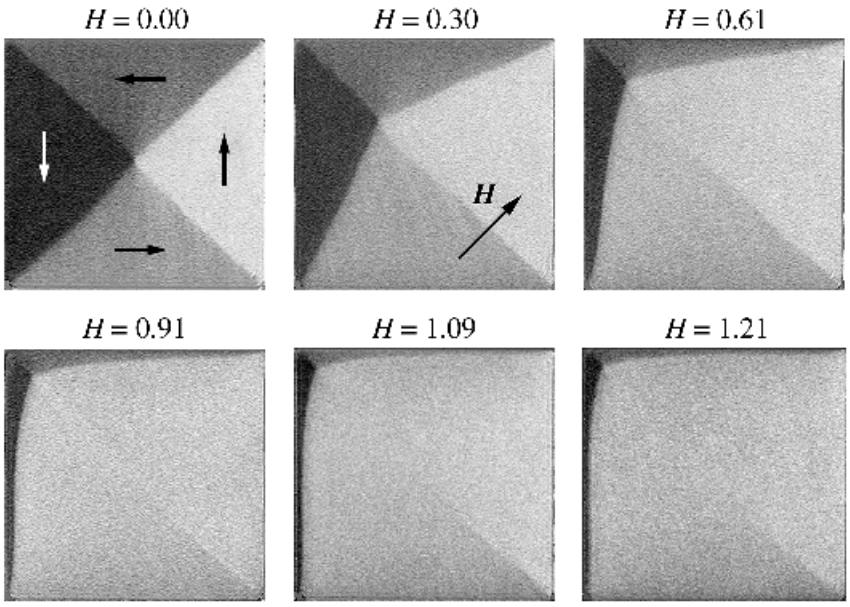


FIGURE 3.3. Permalloy films: $L = 30\ \mu$m, $D = 40$ nm.

[7] Yu Lu, U. Rüdiger, A.D. Kent, L. Thomas, and S.S.P. Parkin, Micromagnetism and magnetization reversal in micron-scale (110) Fe thin-film magnetic elements, Phys. Rev. B **60**, 7352 (1999);

[8] H.A.M. van den Berg, Self–consistent domain theory in soft–ferromagnetic media. II. Basic domain structures in thin film objects, J. Appl. Phys. **60**, 1104 (1986)

[9] P. Bryant and H. Suhl, Thin-film magnetic patterns in an external field, 2224 Appl. Phys. Lett. **54**, 78 and 2224 (1989).

[10] H. Suhl and P. Bryant, The nonlinear horrors of realistic magnetization fields, in: Springer Lecture Notes in Physics **337**, 59 (1989).

[11] M. Rührig, W. Bartsch, M. Vieth, and A. Hubert, Elementary magnetization processes in a low-anisotropy circular thin film disk, IEEE Trans. Magnetics **26**, 2807 (1990).

[12] E. De Giorgi and T. Franzoni, Su un tipo di convergenza variazionale, Atti Accad. Naz. Lincei, Rendiconti Cl. Sc. Mat. Fis. Nat. **58**, 842 (1975).

[13] G. Gioia and R.D. James, Micromagnetics of very thin films, Proc. Roy. Soc. A **453**, 213 (1997).

[14] A. DeSimone, R.V. Kohn, S. Müller, and F. Otto, in preparation.

[15] J.L. Blue and M.R. Scheinfein, Using multipoles decreases computation time for magnetostatic self-energy, IEEE Trans. Magnetics **27**, 4778 (1991).

[16] R.J Vanderbei, *Linear Programming: Foundations and Extensions* (Kluwer, Boston, 1996).

[17] L.C. Evans *Partial Differential Equations* (American Mathematical Society, Providence, 1998), Section 10.1.

[18] J.A. Sethian, *Level Set Methods* (Cambridge University Press, 1996).

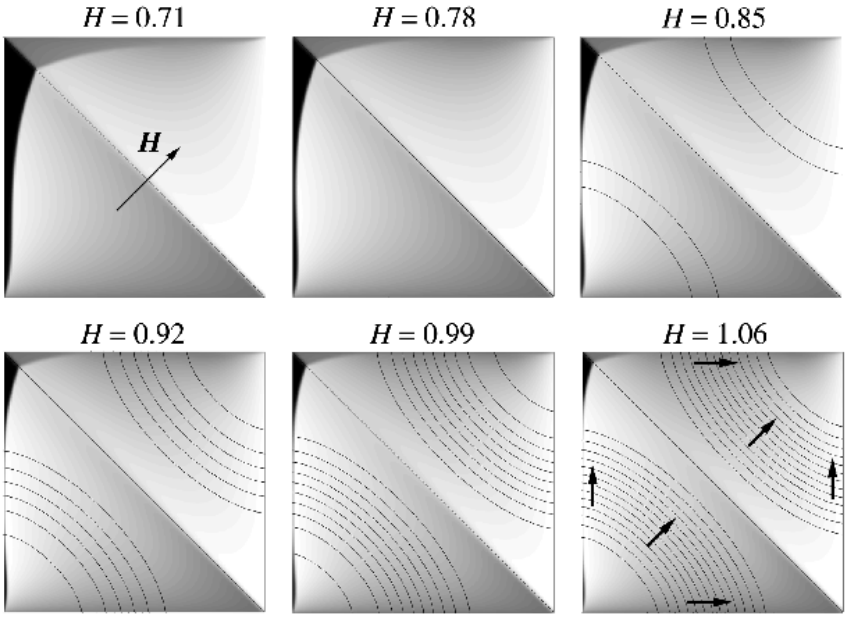


FIGURE 3.4. The transition between expulsion and penetration regimes. Lines show the level curves of the potential of the penetrated field, arrows indicate the magnetization direction.

[19] P. Aviles and Y. Giga, The distance function and defect energy, Proc. Roy. Soc. Edinburgh A **126**, 923 (1996).

[20] W. Jin and R. V. Kohn, Singular perturbation and the energy of folds, J. Nonlinear Science **10**, 355 (2000).

[1]MAX PLANCK INSTITUTE FOR MATHEMATICS IN THE SCIENCES, INSELSTR. 22-26, D-04103 LEIPZIG, GERMANY

[2]COURANT INSTITUTE OF MATHEMATICAL SCIENCES, 251 MERCER ST., NEW YORK, NY 10012

[3]INSTITUT FÜR ANGEWANDTE MATHEMATIK, UNIVERSITÄT BONN, WEGELERSTR. 10, D-53115 BONN, GERMANY

[4]INSTITUT FÜR FESTKÖRPER- UND WERKSTOFFORSCHUNG, HELMHOLTZSTR. 20, D-01069 DRESDEN, GERMANY